J. Fluid Mech. (2015), *vol.* 767, R3, doi:10.1017/jfm.2015.69

JFM RAPIDS
journals.cambridge.org/rapids

Stretching of capsules in an elongation flow, a route to constitutive law

C. de Loubens[1], J. Deschamps[1], G. Boedec[1] and M. Leonetti[1,†]

[1]Aix-Marseille Universite, CNRS, Centrale Marseille, IRPHE UMR 7342, 13384 Marseille, France

(Received 4 November 2014; revised 11 December 2014; accepted 29 January 2015;
first published online 20 February 2015)

Soft bio-microcapsules are drops bounded by a thin elastic shell made of cross-linked proteins. Their shapes and their dynamics in flow depend on their membrane constitutive law characterized by shearing and area-dilatation resistance. The deformations of such capsules are investigated experimentally in planar elongation flows and compared with numerical simulations for three bidimensional models: Skalak, neo-Hookean and generalized Hooke. An original cross-flow microfluidic set-up allows the visualization of the deformed shape in the two perpendicular main fields of view. Whatever the elongation rate, the three semi-axis lengths of the ellipsoid fitting the experimental shape are measured up to 180 % of stretching of the largest axis. The geometrical analysis in the two views is sufficient to determine the constitutive law and the Poisson ratio of the membrane without a preliminary knowledge of the shear elastic modulus G_s. We conclude that the membrane of human serum albumin capsules obeys the generalized Hooke law with a Poisson ratio of 0.4. The shear elastic modulus is then determined by the combination of numerical and experimental variations of the Taylor parameter with the capillary number.

Key words: biological fluid dynamics, capsule/cell dynamics, low-Reynolds-number flows

1. Introduction

Studies on the behaviour in flow of soft particles such as capsules, vesicles and other biomimetic sacs have attracted growing interest in the past decade (Vlahovska, Podgorski & Misbah 2009; Barthès-Biesel 2011; Li, Vlahovska & Karniadakis 2013; Abreu *et al.* 2014). These objects are peculiarly useful in biotechnology to control drug delivery in the human body. Their ability to model some membrane properties of red blood cells (RBCs) (Noguchi & Gompper 2005; Freund 2014; Winkler, Fedosov & Gompper 2014) makes it possible to test each RBC membrane characteristic independently and to investigate the collective motion of RBCs without taking into

† Email address for correspondence: leonetti@irphe.univ-mrs.fr

account the complexity of living cells (Breyiannis & Pozrikidis 2000; Doddi & Bagchi 2009; Lei *et al.* 2013; Zhao & Shaqfeh 2013; Krüger, Kaoui & Harting 2014; Kumar, Henriquez Rivera & Graham 2014).

All of these soft particles share the common characteristic of being drops bounded by a membrane with specific mechanical properties which depend on the kind of constitutive material. Indeed, the membrane of a vesicle is an incompressible bidimensional liquid (a lipid bilayer) with a resistance to bending with no membrane shear elasticity. The membrane of a polymersome is different, as lipids are replaced by copolymers which confers additionally a high shear membrane viscosity. Capsules are very different, as their membranes are made of cross-linked natural or artificial polymers. Their membranes are considered to be 2D elastic solids with a shear and dilatation resistance. However, in fact little is known experimentally on the constitutive law that governs the mechanical response of the membrane to stress, i.e. the relationships between the tensions along the membrane and the local extension ratios. As experiments on capsule membranes are often limited to the determination of the shear elastic modulus in the linear regime, we can only assume the probable existence of several membrane mechanical behaviours. The challenge is to shed light on the nonlinear behaviour of such membranes. For example, a capsule with a membrane made of polysiloxane bursts with minute deformations (4 %, Walter, Rehage & Leonhard 2001), while capsules with a membrane made of cross-linked proteins sustain moderate to intermediate deformations (Risso, Colle-Paillot & Zagzoule 2006; Lefebvre *et al.* 2008) and even huge deformations, as demonstrated in this paper. Two theoretical models have emerged in the community as generic models to study numerically the behaviour of capsules in flow. The Skalak model has been developed to mimic the membrane mechanics of RBCs (Skalak *et al.* 1973) with notably a limit to membrane incompressibility. The bidimensional Neo-Hookean (NH) model, a peculiar case of the Mooney–Rivlin model, has been inspired by results on materials such as rubber (Macosko 1994). These two models have the major and supplementary advantage of describing two kinds of mechanical responses: the strain-hardening behaviour for the Skalak model and the strain softening for the NH model. Consequently, to the best of our knowledge, simulations of the dynamics of capsules in various flows have mainly used these models: elongation flow (Lac *et al.* 2004; Dodson & Dimitrakopoulos 2009; Walter *et al.* 2010; Dimitrakopoulos 2014), shear flow (Ramanujan & Pozrikidis 1998; Bagchi & Kalluri 2009; Vlahovska *et al.* 2011; Yazdani, Kalluri & Bagchi 2011; Dupont, Salsac & Barthès-Biesel 2013; Wang *et al.* 2013), Poiseuille in a capillary (Queguiner & Barthès-Biesel 1997; Pozrikidis 2005) and with a diffuser at the outlet (Zhu *et al.* 2014). Here, we also compute the results using a more elementary model, the generalized Hooke model.

The membrane properties of capsules depend on the fabrication process and notably here on the fact that the membrane results from chemical reactions localized at the interface of an initial drop. The closed geometry brings some constraints to the system which cannot be taken into account by a study on planar membranes. It explains also the continuous development of many techniques to study whole capsules.

However, experimental investigations of capsules in flow are scarce, in contrast to numerical studies. Thus, the nonlinear behaviour of a capsule in an elongation flow has only been studied in the seminal paper of Chang & Olbricht (1993) with a millimetric biphasic capsule with a membrane of nylon. Numerical simulations predict a non-axisymmetric shape which cannot be confirmed by only one view ($z = 0$, figure 1*a*) of the capsule as in the experiment of Chang & Olbricht (1993). In this paper, we propose an original method to image the 3D shape of the capsule, namely the sections of capsules in the planes $z = 0$ and $y = 0$ (figure 1*a*).

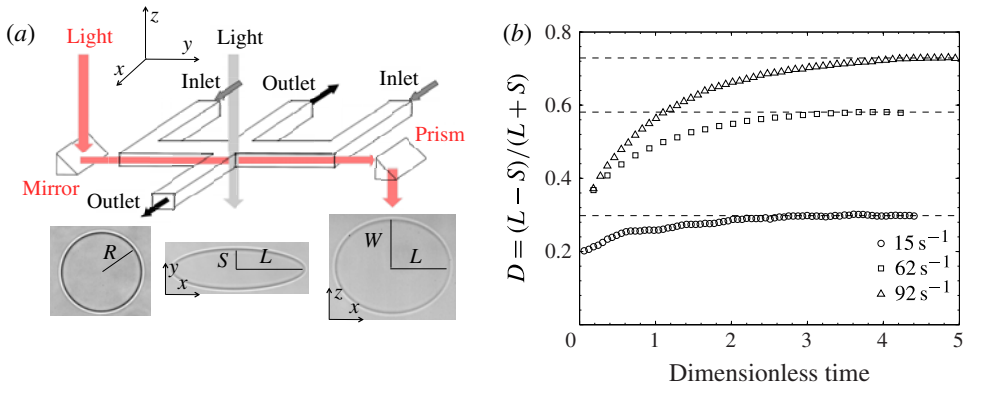

FIGURE 1. Experimental set-up. (*a*) The two perpendicular cross-sections of the deformed capsule at the centre of the cross are visualized by two light paths. A spherical capsule of radius R is deformed by elongation flow and its shape is characterized by its semi-axis length (L, S) in the $z = 0$ plane and (L, W) in the $y = 0$ plane. (*b*) Saturation of the Taylor parameter D with the dimensionless time $\dot{\epsilon}t$ for different elongation rates $\dot{\epsilon}$ on one capsule.

In this paper, we investigate experimentally and numerically the deformation of bio-microcapsules in planar elongation flow. In § 2, the experimental set-up and notably the original optical approach are detailed to provide the way to capture the 3D shape of microcapsules up to 180 % of stretching. The numerical methods are based on the association of the boundary integral method (BIM) with the finite element method (FEM) to take into account the membrane elasticity. In § 3, we show that the large range of deformation in the two planes of deformation allows us to determine unambiguously the constitutive law of the membrane of capsules made of pure human serum albumin (HSA): the generalized Hooke model of known Poisson ratio ν_s. We show also that the shear elastic modulus G_s varies strongly with the capsule size and the HSA concentration, in agreement with recent results (de Loubens *et al.* 2014). The results are highlighted by the excellent agreement – experiments versus numerics – of the variations of the three axes of the shape with the capillary number, validating once more the generalized Hooke model. In § 4, we conclude and discuss the results in the light of the literature.

2. Methods

2.1. *Experimental method*

Microcapsules were prepared by interfacial cross-linking of HSA with terephthaloyl chloride in a water-in-oil emulsion: 15 %–25 % HSA concentration in the drop, C^{3D}_{HSA}, and 1000–1700 r.p.m. stirring speed (Andry, Edwards-Levy & Levy 1996). This leads to various spherical micro-objects embedded in glycerol with radii varying from 30 to 80 μm.

The capsules were deformed in a planar elongational Stokes flow $u_\infty = \dot{\epsilon}(x, -y, 0)$ in the centre of a cross-like channel with a square section of 1 mm^2 (figure 1), where $\dot{\epsilon}$ is the rate of elongation. The fluid was injected through the inlets by a glass syringe mounted on a home-made pump based on a PI M235-52S actuator.

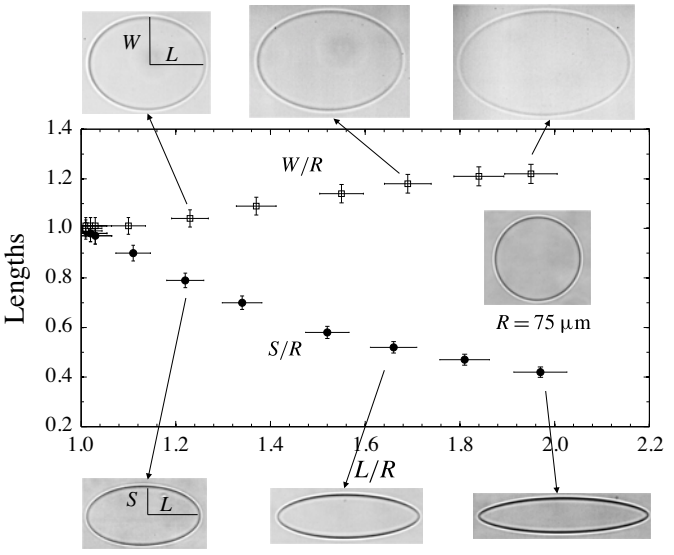

FIGURE 2. Typical variations of S and W versus L for a capsule of radius $R = 75$ μm. The error bars represent ±2 pixels on each length.

The whole system was built in PMMA with the needles sticking inside to prevent a long transient time. The channel was mounted on an inverted Olympus IX-71 microscope with a magnification of $20\times$ (0.851 μm pixel^{-1}).

Chang & Olbricht (1993) have analysed the shape of millimetric biphasic capsules in the view $z = 0$. Here, the two perpendicular cross-sections of the capsule were visualized in $z = 0$ by the classic optical top-down path of the microscope and $y = 0$ by mounting a mirror and a prism to have two collected light paths, see figure 1. Capsule images in the two views and a typical variation of (W, S) with L are provided in figure 2.

A high-speed Photron Fastcam SA3 camera recorded up to 4000 f.p.s. The flow was characterized by particle-tracking velocimetry. The value of $\dot{\epsilon}$ varied from 1 to 500 s^{-1} with a standard deviation below 5 % in a region of 520 μm diameter around the stagnation point; see de Loubens *et al.* (2014) for details. Experiments were carried out at a temperature of 22 ± 0.5 °C controlled with a precision of 0.1 °C. The viscosity of the glycerol, η, ranged from 0.99 to 1.18 Pa s. The time for the flow to reach its stationary value depended only on the pump (≈20 ms) as the viscous time was typically 1 ms. To measure steady small deformations, capsules were trapped one by one at the stagnation point of the channel by regulating the hydrostatic pressure at the outlets and moving the piston of the syringe back and forth as often as necessary. Then, flow was applied. The deformation saturated before the capsule left the field of view (circles in figure 1*b*). To obtain steady high deformations up to 180 %, capsules were trapped one by one at the stagnation point and gently sucked up in one branch of the channel up to 5 mm from the stagnation point. Flow was applied. The capsule was coming from one branch of the channel already deformed and going back by one of the two perpendicular branches in passing by the stagnation point with a saturated dynamics (squares and triangles in figure 1*b*). We checked that these two ways were equivalent for deformations of L up to 60 %. All the capsules returned to their initial spherical shapes and their volumes were constant during the stretching, assuming an

ellipsoidal shape, 5 % of variation in agreement with the experimental errors. Beyond 180 % of stretching, the first results indicated that the capsules break at the tips for $L/R \approx 3$. This study is beyond the scope of this paper.

The three axes of the ellipsoid (L, S, W) were measured as the Taylor parameter $D = (L - S)/(L + S)$. Twenty-five capsules were analysed. All of the following results are reported in the steady state. Each capsule was studied for approximately seven elongation rates. The deformation of the capsules in the flow was characterized by the capillary number Ca, which is defined as the ratio of the hydrodynamic viscous stress $\eta\dot{\epsilon}$ to the elastic response G_s/R, with G_s the surface shear modulus: $Ca = \eta\dot{\epsilon}R/G_s$.

2.2. *Numerical method*

The shapes of the capsules were calculated numerically in elongation flow as a function of Ca in the Stokes flow regime. Far from the capsule, the elongation flow is not perturbed. The membrane is a 2D impermeable (fixed volume) elastic solid involving the continuity of the velocity at the interface. There is no bending resistance, no membrane viscosity and no contrast of fluid viscosity. The mechanical equilibrium involves the balance between the jump of the hydrodynamical stress tensor and the membrane force, which is derived from the surface density energy W^{NH} for the strain-softening NH model, W^{Sk} for the strain-hardening Skalak model and W^{H} for the generalized Hooke model:

$$W^{NH} = \frac{G_s}{2}\left(I_1 - 1 + \frac{1}{1 + I_2}\right), \tag{2.1}$$

$$W^{Sk} = \frac{G_s}{2}\left(I_1^2 + 2(I_1 - I_2) + CI_2^2\right), \tag{2.2}$$

$$W^{H} = \frac{G_s}{4}\left(2(I_1 - I_2) + \frac{1}{1 - \nu_s}I_1^2\right), \tag{2.3}$$

where $I_{1,2}$ are the usual surface strain invariants, ν_s is the surface Poisson ratio ($-1 < \nu_s < 1$) for a 2D material and C is a positive dimensionless parameter: $\nu_s = C/(1 + C)$.

Our simulations are based on the boundary element method (Pozrikidis 2003) for flow resolution, the method used most often for dynamics of soft particles in Stokes flow (Biben, Farutin & Misbah 2011; Boedec, Leonetti & Jaeger 2011; Zhao & Shaqfeh 2011, and references in the introduction). Membrane forces are solved by an FEM for the calculation of membrane forces (Walter *et al.* 2010). The membrane is discretized using Loop subdivision elements (Loop 1987). The number of elements used varies between 1280 for small to 20 480 for large deformations. The relative error on the inner volume conservation is less than 0.05 %. Our simulations with the Skalak and NH models are in excellent agreement with reference results in the literature: see supplementary data 1 available at http://dx.doi.org/10.1017/jfm.2015.69 (Lac *et al.* 2004; Dodson & Dimitrakopoulos 2009; Walter *et al.* 2010; Dimitrakopoulos 2014).

3. Results and discussion

3.1. *Determination of the constitutive law*

Experimentally, the steady-state shape of capsules in elongation flow is non-axisymmetric. In both cross-sections, the shape is an ellipse but with different small axis (S, W): S decreases while W increases with the stretching (figure 2). However, W/R deviates from the resting state value (i.e. from 1 to at least 1.05) for L/R

larger than 1.3. The linear variation of S with L and the small change of W in the limit of small deformations ($L/R < 1.1$) are in agreement with asymptotic theories (Barthès-Biesel, Diaz & Dhenin 2002). At the highest level of deformation ($L/R \approx 2.8$ which corresponds to a stretching of 180 %), S decreases by 70 % and W increases by 30 %. Hence, the maximal stretches of the perimeters of the ellipses in the planes $z = 0$ and $y = 0$ are respectively 270 % and 310 %. These large deformations constitute the key differences from previous experiments where the dilatation of the perimeter of capsules moving in a capillary was limited to 20 % (Risso *et al.* 2006; Lefebvre *et al.* 2008) or the radial extension of compressed capsules was less than 30 % (Carin *et al.* 2003). If A is the area of the capsule and A_o is its value in the resting state, A/A_o varies from 1 to 1.2 (20 %) for $L/R = 1.6$ and to 1.8 (80 %) for $L/R = 2.5$. Finally, small, moderate and high deformations can be defined as $L/R < 1.1$, $L/R < 1.4$ and $L/R > 1.4$.

Remarkably, whatever the initial concentration of proteins in the drops and the size of the capsules, all the deformations follow master curves considering the smaller lengths S/R and W/R as functions of the largest one L/R, see figure 3. The deviation between the capsules is less than approximately 5 % for similar values of L/R. We emphasise that there is no fitting parameter and no preliminary knowledge of the shear elastic modulus to collapse the experimental data. As we will demonstrate in the following, this purely geometrical analysis and the large deformation allow us to conclude unambiguously on the constitutive law by comparing experimental data with numerical curves.

Consider the classic view $z = 0$, i.e. the visualization used in previous experiments on drops, vesicles and capsules (Chang & Olbricht 1993; Stone 1994; Kanstler, Segre & Steinberg 2007). For $L/R < 1.8$, the Skalak, NH and Hooke models are in agreement with the experimental data if the fitting parameter C of the Skalak model is well chosen: $C \approx 0.5$. At larger deformations, the Hooke and NH results are still in agreement with experiments. However, the curve S as a function of L, for $C = 0.5$, differs from the master curve satisfied by the experimental results (figure 3*a*). This comparison shows that if this view cannot completely discriminate the models, the Skalak numerical curves are very sensitive to the parameter C of the model depending on the regime of deformations.

Consider the perpendicular view $y = 0$ visualized for the first time (figure 3*b*). At large stretching, the numerical results differ markedly. In the Skalak model, W increases as a function of L and has a maximum that corresponds to $L/R = 1.8$ (2.1) for $C = 0.5$ (0.25). The experimental data do not show any maximum; W/R increases with the stretching without saturation which differs from the decrease of W/R at very large stretching for the Skalak model. This comparison allows us to exclude the Skalak model for HSA microcapsules. The numerical curve obtained with the NH model crosses the experimental data ($1.9 < L/R < 2$). At low (large) stretching, the NH results overestimate (underestimate) W/R. The slope of W versus L is clearly different between experiments and NH simulation, contrary to the Hooke model. Thus, even if the qualitative trend is correct, the NH model does not describe quantitatively the deformations of capsules, contrary to the Hooke model.

It is possible to go further, considering now the hydrodynamic stress $\eta\dot{\epsilon}$. The ratio $L/R\eta\dot{\epsilon}$ decreases continuously when L increases for the Hooke model, whereas this ratio saturates and increases weakly at larger stretching for the NH model (figure 3*c*). The experimental results differ markedly from the NH curve and are in excellent agreement with the Hooke curve. We conclude that the generalized Hooke model with a Poisson ratio $\nu_s = 0.4 \pm 0.1$ is the most relevant to describe the experimental results for HSA microcapsules.

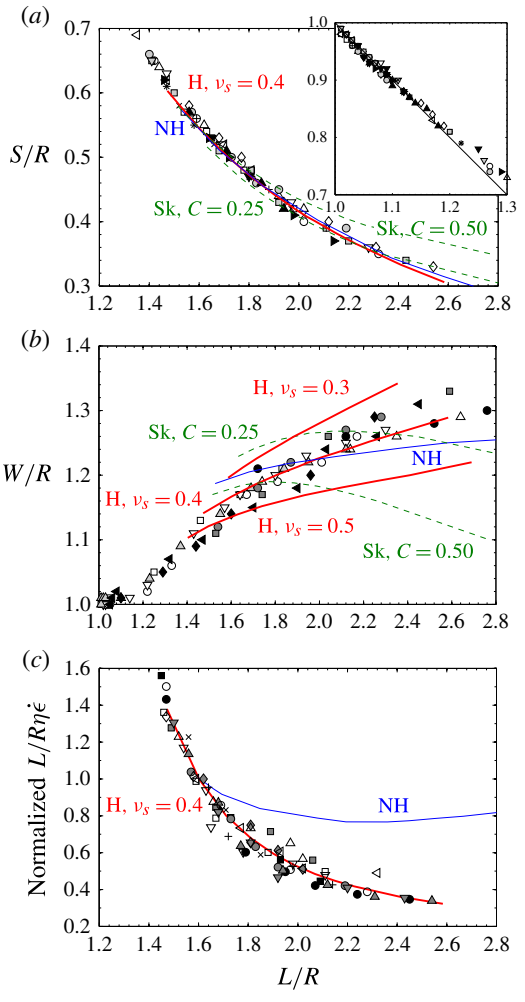

FIGURE 3. Variation of the characteristic lengths S/R, W/R and $(L/R\eta\dot{\epsilon})/(L/R\eta\dot{\epsilon})_{L/R=1.6}$ as a function of L/R in elongation flow. Symbols are for experimental results and curves for numerical ones, with H for the generalized Hooke model (bold line), Sk for the Skalak model (dashed line) and NH for the NH model. Here, ν_s is the surface Poisson coefficient for H and C is a parameter of Sk. Errors correspond to approximately $\pm 5\,\%$ on the half-length W/R. Each symbol corresponds to one capsule stretched by several different elongation rates. Numerical simulations are available in supplementary data 2.

3.2. *Deformations with the capillary number: the shear elastic modulus*

Now that the relevant elastic model has been established, the variation of the Taylor parameter $D = (L - S)/(L + S)$ with Ca is calculated numerically (figure 4*a*). For each studied capsule, experiments provide the values of D for approximately seven different elongation rates. For each capsule, the experimental data set is collapsed onto the numerical curve using the last free parameter, the shear elastic modulus G_s. The error of the regression is less than 10 %. The value of G_s ranged from 0.7 to 16.6 mN m^{-1} (figure 5). As observed in the linear regime (de Loubens *et al.* 2014), G_s increases with the initial concentration of proteins, C^{3D}_{HSA}, and the size of the capsules, which

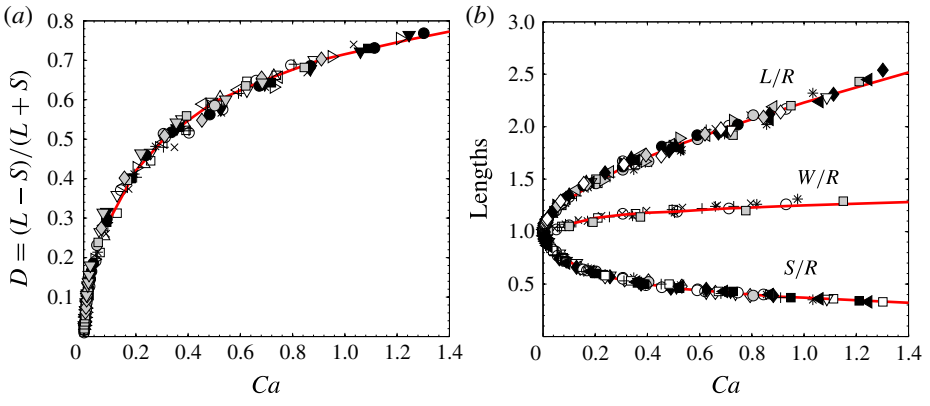

FIGURE 4. Deformation as a function of the capillary number Ca. (a) The fitting of the experimental data on the numerical master curve $D = f(Ca)$ for the Hooke law and a Poisson coefficient of 0.4 provides the shear elastic modulus G_s. (b) Comparison of the experimental and numerical evolution of the three main axes with Ca. Each symbol corresponds to one capsule stretched by several different elongation rates. Numerical simulations are available in supplementary data 2.

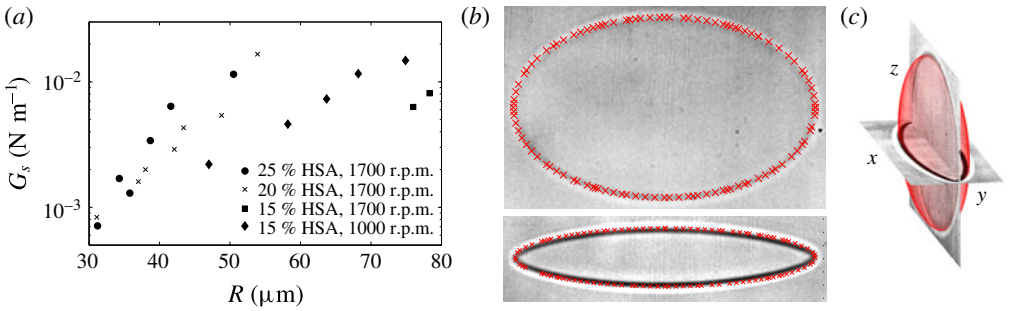

FIGURE 5. (a) Shear elastic modulus as a function of the radius R and the HSA concentration. (b) Capsule profiles compared with numerical simulation (red) for the Hooke model in $y = 0$ (top) and $z = 0$ (bottom). The capsule has a radius of 47 μm and a stretching L/R of 2. (c) The same highly deformed capsule image with experimental and 3D numerical profiles highlights the unexpected flatness of the tri-axial ellipsoid shape. A high-resolution image is available in supplementary data 3.

questions the physical mechanisms involved during the process of cross-linking of the membrane (Gunes *et al.* 2011). In a first approximation assuming a total reaction at the interface, the increasing HSA concentration of the membrane $C^{2D}_{HSA} \approx R\, C^{3D}_{HSA}/3$ with R and C^{3D}_{HSA} supports the observed variations.

Finally, it is possible to compare experimental and numerical variations of the semi axes (L, S, W) with the capillary number (figure 4b). It is noteworthy that the agreement is excellent, supporting once again the generalized Hooke model and the self-consistency of our approach. The dispersion around the numerical simulations is less than ±3 %.

3.3. *Discussion*

To the best of our knowledge, Lefebvre *et al.* (2008) were the first to investigate the constitutive law of capsules experimentally. They concluded that membranes made of albumin obey an NH model by studying the deformation of a capsule inside a narrow capillary. We expected the same for our study on HSA capsules, as the method of fabrication is the same and the proteins are of the same family. What could be the origin of this discrepancy? On the one hand, the two proteins differ markedly by their number of amino acids, as illustrated by their molar masses, 45 kDa and 66 kDa for ovalbumin and HSA respectively. Moreover, the purity of the ovalbumin used was approximately 70 % (Sigma-Aldrich, A5253), while in our study the HSA was pure at 98 %. These two elements might make the comparison questionable. On the other hand, Lefebvre *et al.* (2008) only used the Skalak and NH models to compare experiments with simulations. The generalized Hooke model could describe their experimental results inside a capillary more properly. Further investigations of both the deformation of ovalbumin capsules in an elongation flow and the comparison with the numerical profiles deduced from the Hooke model of axisymmetric capsules moving along a capillary seem to be necessary to clarify the constitutive law of ovalbumin capsules.

4. Conclusion

The behaviour of soft bio-microcapsules in elongation flow has been studied up to the nonlinear regime just before bursting. By a combination of experimental and numerical investigations, we determined unambiguously the constitutive law (or strain–energy) that governs the mechanics of a capsule membrane made of HSA, namely the bidimensional generalized Hooke model. This method could be applied to all capsules that support large stretching, to distinguish clearly the 2D membrane elastic models. Capsules made of chitosan and cross-linked proteins should be good candidates. By extension, this method might be applicable to a wide range of soft particles. In contrast, it needs to be improved for stiffer membranes, with a feedback to maintain the capsule for a longer time at the stagnation point.

Bending resistance was not necessary to capture the overall shape of our capsules with the Hooke model. Indeed, the comparison between the experimental and numerical profiles shows excellent agreement, see figure 5(*b*). It should be noted that the 3D comparison highlights the unexpected flatness of the tri-axial ellipsoidal shape of a capsule in the high-deformation regime, see figure 5(*c*) and supplementary data 3. For a small resistance to bending, we could expect localized contributions at the tips or along the membrane in the form of wrinkles in the moderate regime of deformations for which no stationary numerical solution exists (Finken & Seifert 2006). However, we did not observe any effect on the studied capsules made of HSA. However, if wrinkles are not deep, they could only be seen in the $x = 0$ plane, an open issue. In the regime of high deformation studied here, the shear and dilatational elastic energy dominates the bending energy. More generally, our general method based on the deformation of a capsule in an elongation flow and the comparison experiments versus numerical simulations should be valid whatever the resistance to bending.

Finally, the robustness of our conclusions was achieved by combining a novel set-up that visualizes the two perpendicular cross-sections of capsules, a range of high capillary numbers and the softness of these capsules associated with numerical simulations. These conditions can be fulfilled in many configurations of flow. A good candidate is the study of the shape dynamics of HSA capsules in a shear flow.

Acknowledgements

We thank F. Edwards-Lévy for the preparation of microcapsules and details on ovalbumin and HSA. This work has benefited from financial support from the ANR CAPSHYDR (11-BS09-013-02), from Labex MEC (ANR-11-LABX-0092), from A*MIDEX (ANR-11-IDEX-0001-02) and from CNES. This work was granted access to the HPC resources of Aix-Marseille Université financed by the project Equip@Meso (ANR-10-EQPX-29-01).

Supplementary data

Supplementary data is available at http://dx.doi.org/10.1017/jfm.2015.69.

References

ABREU, D., LEVANT, M., STEINBERG, V. & SEIFERT, U. 2014 Fluid vesicles in flow. *Adv. Colloid Interface Sci.* **208**, 129–141.

ANDRY, M. C., EDWARDS-LEVY, F. & LEVY, M. C. 1996 Free amino group content of serum albumin microcapsules. III. A study at low pH values. *Intl J. Appl. Pharmacol.* **128**, 197–202.

BAGCHI, P. & KALLURI, R. M. 2009 Dynamics of nonspherical capsules in shear flow. *Phys. Rev.* E **80**, 016307.

BARTHÈS-BIESEL, D. 2011 Modeling the motion of capsules in flow. *Curr. Opin. Colloid Interface Sci.* **16**, 3–12.

BARTHÈS-BIESEL, D., DIAZ, A. & DHENIN, E. 2002 Effect of constitutive laws for two-dimensional membranes on flow-induced capsule deformation. *J. Fluid Mech.* **460**, 211–222.

BIBEN, T., FARUTIN, A. & MISBAH, C. 2011 Three-dimensional vesicles under shear flow: numerical study of dynamics and phase diagram. *Phys. Rev.* E **83**, 031921.

BOEDEC, G., LEONETTI, M. & JAEGER, M. 2011 3D vesicle dynamics simulations with a linearly triangulated surface. *J. Comput. Phys.* **230**, 1020–1034.

BREYIANNIS, G. & POZRIKIDIS, C. 2000 Simple shear flow of suspensions of elastic capsules. *J. Theor. Comput. Fluid Dyn.* **13**, 327–347.

CARIN, M., BARTHÈS-BIESEL, D., EDWARDS-LÉVY, F., POSTEL, C. & ANDREI, D. C. 2003 Compression of biocompatible liquid-filled HSA-alginate capsules: determination of the membrane mechanical properties. *Biotechnol. Bioengng* **82**, 207–212.

CHANG, K. S. & OLBRICHT, W. 1993 Experimental studies of the deformation of a synthetic capsule in extensional flow. *J. Fluid Mech.* **250**, 587–608.

DIMITRAKOPOULOS, P. 2014 Effects of membrane hardness and scaling analysis for capsules in planar extensional flows. *J. Fluid Mech.* **745**, 487–508.

DODDI, S. K. & BAGCHI, P. 2009 Three-dimensional computational modeling of multiple deformable cells flowing in microvessels. *Phys. Rev.* E **79**, 046318.

DODSON, W. R. III & DIMITRAKOPOULOS, P. 2009 Dynamics of strain-hardening and strain-softening capsules in strong planar extensional flows via an interfacial spectral boundary element algorithm for elastic membranes. *J. Fluid Mech.* **641**, 263–296.

DUPONT, C., SALSAC, A.-V. & BARTHÈS-BIESEL, D. 2013 Off-plane motion of a prolate capsule in a shear flow. *J. Fluid Mech.* **721**, 180–198.

FINKEN, R. & SEIFERT, U. 2006 Wrinkling of microcapsules in shear flow. *J. Phys.: Condens. Matter* **18**, L185–L191.

FREUND, J. B. 2014 Numerical simulation of flowing blood cells. *Annu. Rev. Fluid Mech.* **46**, 67–95.

GUNES, D. Z., POUZOT, M., ULRICH, S. & MEZZENGA, R. 2011 Tuneable thickness barriers for composite o/w and w/o capsules, films, and their decoration with particles. *Soft Matt.* **7**, 9206–9215.

KANSTLER, V., SEGRE, E. & STEINBERG, V. 2007 Vesicle dynamics in time-dependent elongation flow: wrinkling instability. *Phys. Rev. Lett.* **99**, 178102.

KRÜGER, T., KAOUI, B. & HARTING, J. 2014 Interplay of inertia and deformability on rheological properties of a suspension of capsules. *J. Fluid Mech.* **751**, 725–745.

KUMAR, A., HENRIQUEZ RIVERA, R. G. & GRAHAM, M. D. 2014 Flow-induced segregation in confined multicomponent suspensions: effects of particle size and rigidity. *J. Fluid Mech.* **738**, 423–462.

LAC, E., BARTHÈS-BIESEL, D., PELEKASIS, N. & TSAMOPOULOS, J. 2004 Spherical capsules in three-dimensional unbounded Stokes flows: effect of the membrane constitutive law and onset of buckling. *J. Fluid Mech.* **516**, 303–334.

LEFEBVRE, Y., LECLERC, E., BARTHÈS-BIESEL, D., WALTER, J. & EDWARDS-LÉVY, F. 2008 Flow of artificial microcapsules in microfluidic channels: a method for determining the elastic properties of the membrane. *Phys. Fluids* **20**, 123102.

LEI, H., FEDOSOV, D. A., CASWELL, B. & KARNIADAKIS, G. EM. 2013 Blood flow in small tubes: quantifying the transition to the non-continuum regime. *J. Fluid Mech.* **722**, 214–239.

LI, X., VLAHOVSKA, P. M. & KARNIADAKIS, G. E. 2013 Continuum- and particle-based modeling of shapes and dynamics of red blood cells in health and disease. *Soft Matt.* **9**, 28–37.

LOOP, C. 1987 *Smooth Subdivision Surfaces Based on Triangles*. University of Utah.

DE LOUBENS, C., DESCHAMPS, J., GEORGELIN, M., CHARRIER, A., EDWARDS-LÉVY, F. & LEONETTI, M. 2014 Mechanical characterization of cross-linked serum albumin microcapsules. *Soft Matt.* **10**, 4561–4568.

MACOSKO, C. 1994 *Rheology: Principles, Measurements and Applications*. Wiley-VCH.

NOGUCHI, H. & GOMPPER, G. 2005 Shape transitions of fluid vesicles and red blood cells in capillary flows. *Proc. Natl Acad. Sci. USA* **102**, 14159–14164.

POZRIKIDIS, C. 2003 *Numerical Simulation of Cell Motion in Tube Flow*. Chapman & Hall.

POZRIKIDIS, C. 2005 Modeling and simulation of capsules and biological cells. *Ann. Biomed. Engng* **33**, 165–178.

QUEGUINER, C. & BARTHÈS-BIESEL, D. 1997 Axisymmetric motion of capsules through cylindrical channels. *J. Fluid Mech.* **348**, 349–376.

RAMANUJAN, S. & POZRIKIDIS, C. 1998 Deformation of liquid capsules enclosed by elastic membranes in simple shear flow: large deformations and the effect of fluid viscosities. *J. Fluid Mech.* **361**, 117–143.

RISSO, F., COLLE-PAILLOT, F. & ZAGZOULE, M. 2006 Experimental investigation of a bioartificial capsule flowing in a narrow tube. *J. Fluid Mech.* **547**, 149–173.

SKALAK, R., TOZEREN, A., ZARDA, R. P. & CHIEN, S. 1973 Strain energy function of red blood cell membranes. *Biophys. J.* **13**, 245–264.

STONE, H. 1994 Dynamics of drop deformation and breakup in viscous fluids. *Annu. Rev. Fluid Mech.* **25**, 65–102.

VLAHOVSKA, P. M., PODGORSKI, T. & MISBAH, C. 2009 Vesicles and red blood cells in flow: from individual dynamics to rheology. *C. R. Acad. Sci. Paris* **10**, 775–789.

VLAHOVSKA, P. M., YOUNG, Y.-N., DANKER, G. & MISBAH, C. 2011 Dynamics of a non-spherical microcapsule with incompressible interface in shear flow. *J. Fluid Mech.* **678**, 221–247.

WALTER, A., REHAGE, H. & LEONHARD, H. 2001 Shear induced deformation of microcapsules: shape oscillations and membrane folding. *Colloids Surf.* A **123**, 183–185.

WALTER, J., SALSAC, A.-V., BARTHÈS-BIESEL, D. & LE TALLEC, P. 2010 Coupling of finite element and boundary integral methods for a capsule in a Stokes flow. *Intl J. Numer. Meth. Engng* **83**, 829–850.

WANG, Z., SUI, Y., SELT, P. D. M. & WANG, W. 2013 Three-dimensional dynamics of oblate and prolate capsules in shear flow. *Phys. Rev.* E **88**, 053021.

WINKLER, R. G., FEDOSOV, D. A. & GOMPPER, G. 2014 Dynamical and rheological properties of soft colloid suspensions. *Curr. Opin. Colloid Interface Sci.* **19**, 594–610.

YAZDANI, A. Z. K., KALLURI, R. M. & BAGCHI, P. 2011 Tank-treading and tumbling frequencies of capsules and red blood cells. *Phys. Rev.* E **83**, 046305.

ZHAO, H. & SHAQFEH, E. S. G. 2011 The dynamics of a vesicle in simple shear flow. *J. Fluid Mech.* **674**, 578–604.

ZHAO, H. & SHAQFEH, E. S. G. 2013 The dynamics of a non-dilute vesicle suspension in a simple shear flow. *J. Fluid Mech.* **725**, 709–731.

ZHU, L., RORAL, C., MITRA, D. & BRANDT, L. 2014 A microfluidic device to sort capsules by deformability: a numerical study. *Soft Matt.* **10**, 7705–7711.